

Supplementary information for

Protein Nanorings Organized by poly(styrene-*block*-ethylene glycol) self-assembled thin films

Jenny Malmström^{1,2*}, Akshita Wason³, Fergus Roache^{1,2}, N. Amy Yewdall⁴, Mazdak Radjainia⁵, Shanghai Wei⁶, Michael J. Higgins⁷, David E. Williams^{1,2}, Juliet A. Gerrard^{1,5} and Jadranka Travas-Sejdic^{1,2}

¹MacDiarmid Institute for Advanced Materials and Nanotechnology, New Zealand

²Polymer Electronics Research Centre, School of Chemical Sciences, University of Auckland, New Zealand

³Department of Chemistry, University of Canterbury, New Zealand

⁴School of Biological Sciences, University of Canterbury, New Zealand

⁵School of Biological Sciences and School of Chemical Sciences, University of Auckland, New Zealand

⁶Department of Chemical and Materials Engineering, University of Auckland, New Zealand

⁷ARC Centre of Excellence for Electromaterials Science, Intelligent Polymer Research Institute, University of Wollongong, NSW, Australia

PEGylation of Lsm α ring

In order to solubilize the Lsm α protein in the spincoating polymer mixture, the protein was PEGylated. The PEG-chains serve to provide a hydrophilic matrix around the protein, which captures water and protects the protein in the benzene spincoating mixture. As the Lsm α protein consists of seven subunits in a ring, stabilized by hydrogen bonding and hydrophobic interactions, it is important that the PEG-chains are not too long in order to not disrupt the tertiary and quaternary structure of the protein. After PEGylation, the protein was purified by size exclusion chromatography and analyzed by SDS-page electrophoresis. It was seen that 5 kDa PEG chains disrupted the protein structure (data not shown), while 2 kDa PEG chains allowed for maintenance of the proteins structure (see figure 1 for size exclusion chromatography and SDS-PAGE), while allowing for solubilization of the protein in the solvent mixture used.

There are three lysines per Lsm α monomer, of which 1 is surface exposed¹. Three PEGylated lysines/monomer gives an expected mass of ~15 kDa per monomer or ~100 kDa for the ring, while one PEGylated lysine would result in a monomer mass of 11 kDa and a mass of 77 kDa for the ring. Experimentally, the shift in elution volume from the size exclusion column corresponding to a mass of the doughnut of 63 kDa before and 240 kDa after pegylation, which indicates aggregation of higher order structures, but is expected to also relate to the larger hydrodynamic radius of PEG (per molecular weight) compared to protein², the column in this case was calibrated using Biorad Gel Filtration standard.

SDS-PAGE reveals an increase in monomer mass of approximately 8 kDa, and an observed mass of the ring species around 90 kDa, both indicating PEGylation of more than one lysine per monomer, but the exact PEGylation is difficult to determine due to well-known interactions between PEG and SDS^{2,3}. The ring shaped structure of Lsm α before and after PEGylation was confirmed by TEM of the protein deposited onto a carbon coated copper grid, negative stained with uranyl acetate (Figure S1 c-d). This provides further evidence of that the PEGylation does not disrupt the multimeric protein interactions in the ring. Interestingly, the PEGylated protein ring was also seen to be SDS stable, and not to break down into smaller oligomeric units like the native structure (Figure S1b, lane 1, 40 kDa).

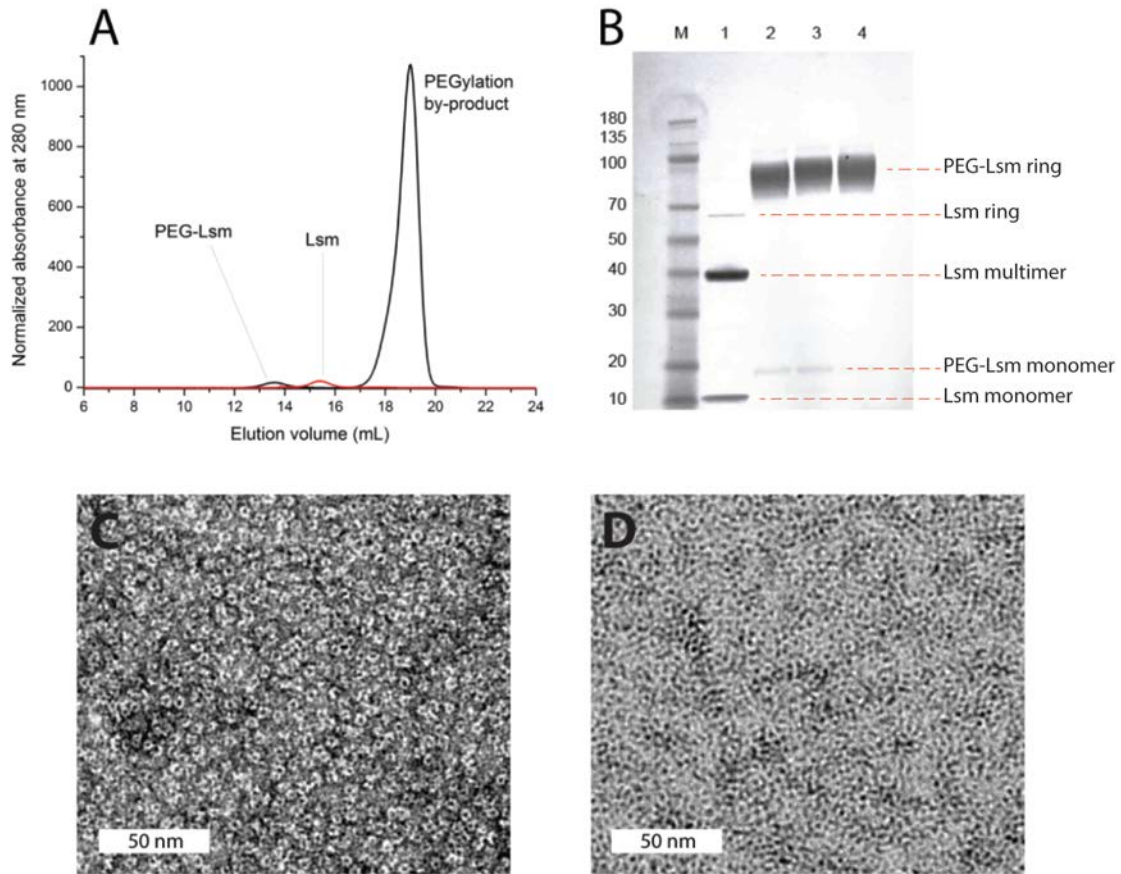


Figure S1: A) Size exclusion chromatography trace of native Lsm α protein (red) and PEGylated-Lsm α (black). The peak at ~19 ml shows the hydrolysed product. Native Lsm α elutes at 15 ml corresponding to ~63 kDa. The PEG-Lsm α elutes at ~13 ml corresponding to ~240 kDa. B) SDS-PAGE gel of native Lsm α (lane 1) and PEGylated samples (lanes 2-4). The monomer shifts from ~10 kDa to ~18 kDa. The PEGylated samples are observed at ~90 kDa. The marker (M) is in kDa. C) TEM image of Lsm α before and after (D) PEGylation.

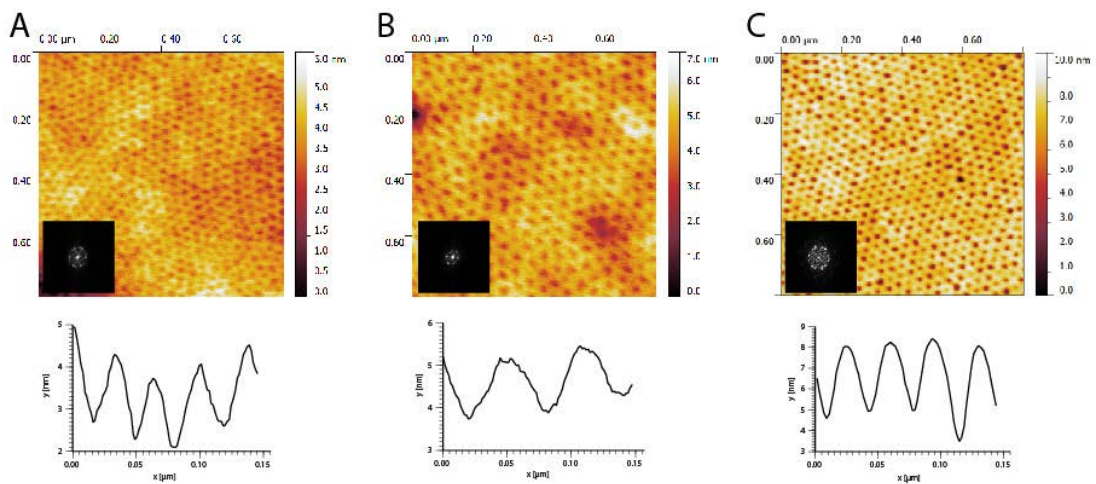


Figure S2: AFM of PS-b-PEO without (a) and with (b) protein (Lsm α PEG) redisplayed from figure 1 as comparison with (c), which shows PS-b-PEO blended with PEO homopolymer. The films were deposited and annealed on gold using identical conditions. 2D FFT insert is $0.2\mu\text{m}^{-1}$ wide in all figures.

The control sample prepared with free PEG (same weight as PEGylated protein used to prepare protein containing films) in figure S2c, shows a slight expansion of the lattice spacing as expected, but not to the same extent as the protein containing sample. The apparent depth of PEO domains is also larger than in Figure S2a-b. This may indicate that the PEO is in fact crystallized in the case of homopolymer addition (also indicated by the phase contrast), but effects of imaging conditions and tip shape between the images cannot be ruled out. The high ordering in S2c, but clear grain boundary, gives rise to discrete double spots in the power spectrum, relating to the direction of each grain.

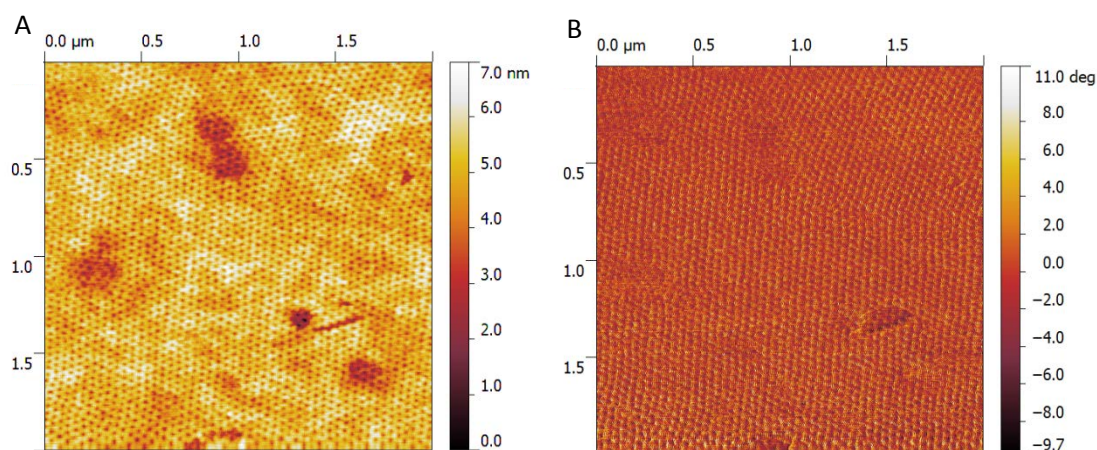


Figure S3: Height (A) and phase (B) of PS-b-PEO (control solvent) on gold coated wafer.

X-Ray photoelectron spectroscopy

The XPS spectra show the expected oxygen and carbon from the polymer, and a weak signal from the underlying gold substrate – most likely from pin holes or other defects. Calculations based solely on the stoichiometry of the polymer mass (from molecular weight the repeating units are as follows: S_{173} -b- EO_{170}) leads to an expected mole fraction of 9.9% oxygen, while the observed values are significantly lower. Due to the surface sensitivity of XPS, this may be explained in terms of adventitious carbon contamination, but could also be a result of how the different blocks of the polymer are exposed to the surface. Interestingly though, the ratio of carbon relating to the PEO (C-O-C) and PS (C-C) derived from the peak fitting (in accordance with reference⁴) to the high resolution C1s spectra is well aligned with the expected values. For the protein containing film, one would expect a nitrogen signal, providing the protein is close enough to the surface to be sampled. However, this could not be detected in any case (2 samples, 3 spots on each sample), which shows that either the protein is not present in the sample at a level that can be detected, or the protein is not exposed to the surface of the film but buried within the PEO domains (as expected). In fact, both the O/C ratio (≈ 0.04) and the assigned carbon components from the high resolution spectra (figure 3a,b) are the same for the film with and without protein. As a reference, XPS was also recorded for freeze-dried $LSm\alpha$ -powder (not PEGylated), which displayed protein characteristic carbon components assigned in figure 3c, of which the C=O(N) component at 288.3 eV⁵ is unique to the protein and not seen in the protein containing polymer film. Thus, it is confirmed to not be the lower sensitivity of nitrogen that caused the absence of protein detection. One difference can be seen in the ratio of the C-O-C component versus the aliphatic and aromatic carbons. This ratio increases from 22% to 26% with protein incorporation. This may relate to the expansion of the PEO domains (seen by AFM, figure 1) upon protein inclusion, even if the protein itself is not detected. After

leaching of the protein containing film by exposing the sample to a drop of water followed by slow evaporation of the drop, the protein can be clearly detected on top of the sample by XPS (see presence of nitrogen in the elemental composition in table S1, and protein unique C=O(N) component in figure S4d). It is worth noting that the C-N and C-O-C components overlap and that the assignment of aliphatic versus aromatic carbon may be of less relevance after the leaching. The Lsm α powder (freeze dried from buffer) display a large amount of sodium, and sodium is also clearly still associated with the protein incorporated in the film as seen by the sodium signal that arises after leaching. This is more sodium than expected, but sodium ions are known to associate with proteins and are often seen in, for example, electrospray ionization mass spectra of protein samples that have been exposed to sodium ions.⁶ Despite the visible potassium signal (K_{2p}) in the C_{1s} region, potassium was not detected at a significant level in the survey spectra.

Table S1: Chemical composition in atom % determined by XPS. The peak used for the quantification is indicated in the table.

Sample	O 1s(%)	C 1s(%)	N 1s(%)	Au 4f(%)	Na 1s(%)	Cl 2p	other
PS-b-PEO	3.73 ± 0.81	95.6 ± 0.79	-	0.67 ± 0.06	-		
PS-b-PEO Lsm α PEG	3.47 ± 0.70	95.8 ± 0.69	-	0.69 ± 0.13	-		
Expected PS-b-PEO (bulk)	9.9	90.1	-	-	-		
Lsm α powder	17.7	39.2	5.34	-	27.9	8.05	1.82 ⁱ
PS-b-PEO Lsm α PEG leached	23.4 ± 0.36	61.6 ± 0.16	7.6 ± 0.1		7.4 ± 0.3		

Table S2: Quantification of carbon components assigned to narrow C1s scans.

Sample	C=O(N) (%)	C-N (%)	C _{C-O-C} (%)	C _{aromatic}	C _{aliphatic} (%)	C-O-C/(C _{other}) (%)
PS-b-PEO	-	-	18.3	61.3	20.4	22
PS-b-PEO Lsm α PEG	-	-	20.5	59.6	19.9	26
Expected (bulk)	-	-	19.7	60.2	20.1	24.6
Lsm α powder	15.1	18.8		66.0		
PS-b-PEO Lsm α PEG leached	9.46	28.5		46.6	15.5	

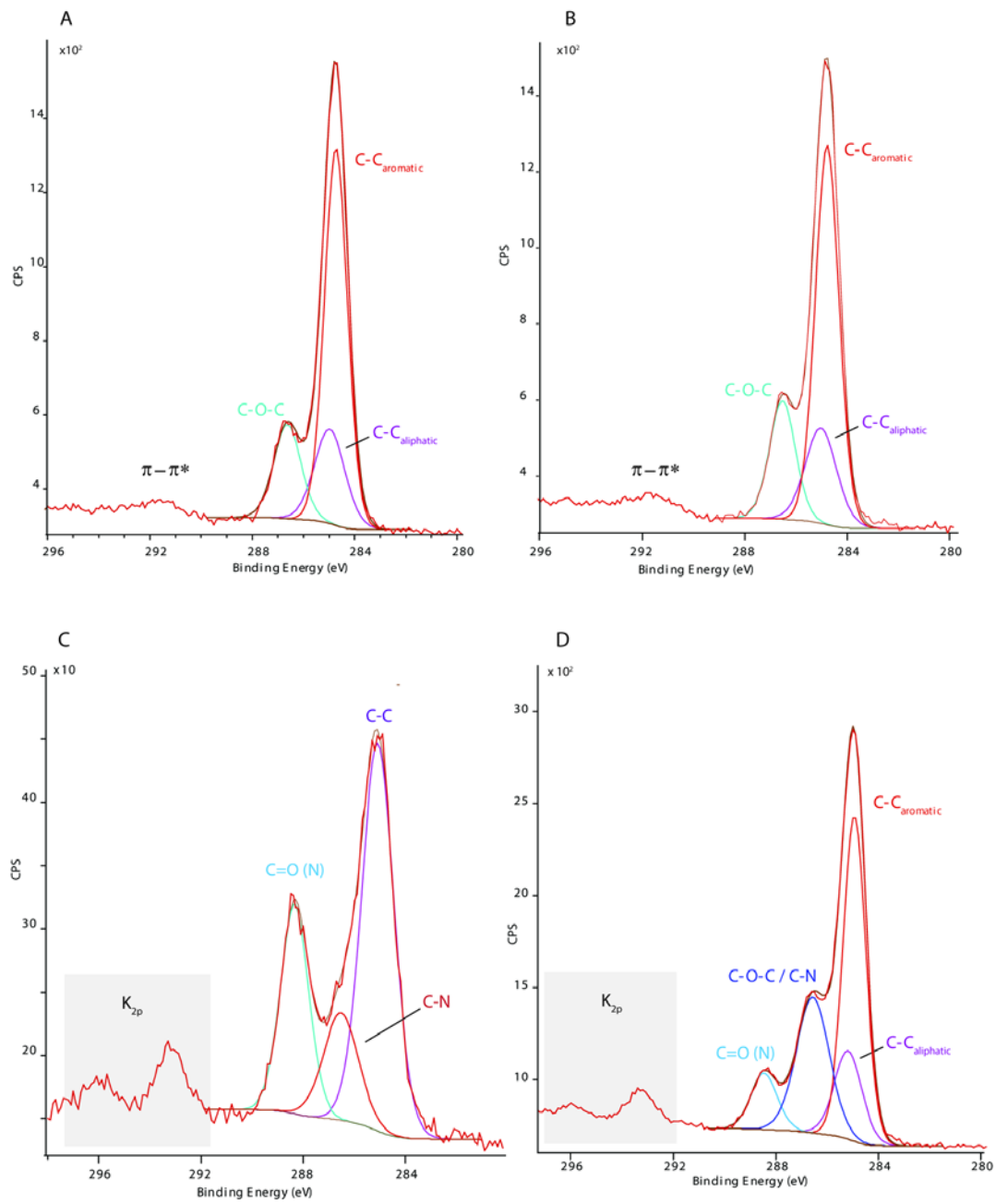


Figure S4: High resolution C1s XPS spectra of A) PS-b-PEO, B) PS-b-PEO Lsm α PEG C) Lsm α powder and D) PS-b-PEO Lsm α PEG after leaching.

Liquid imaging of PS-b-PEOLs α PEG

PBS was added to sample and the first image was acquired after 11 minutes. The phase indicates that imaging is done in the attractive regime. The figures below show a time sequence after addition of PBS, with the first image in Figure S6 (1 μm scan), and following images in figure S7 (500 nm scans) and figure S8 (1 μm scans), where the scan area is offset slightly between figure S7 and S8 to ensure the effect was not due to damage occurring from the imaging.

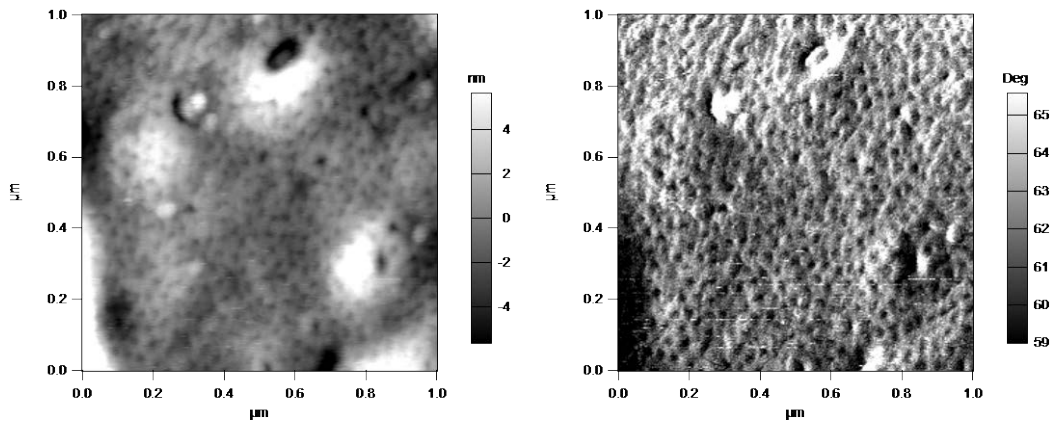
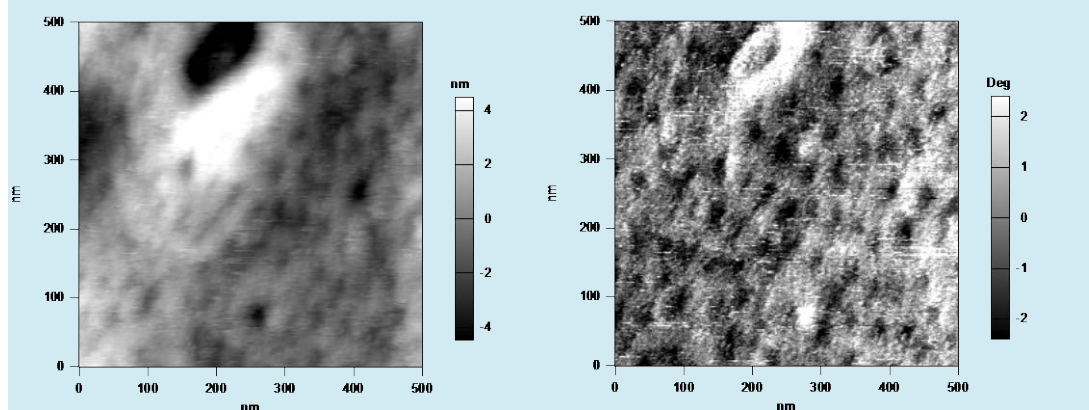


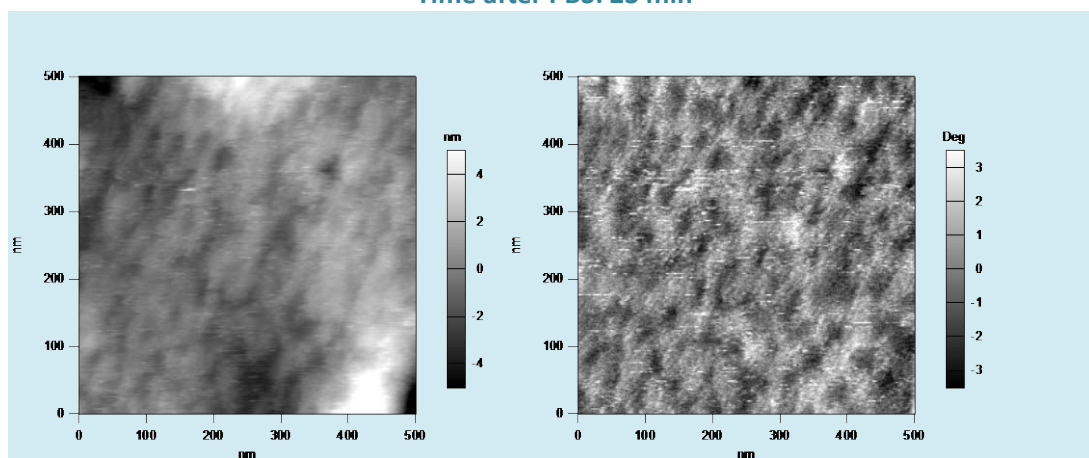
Figure S6: Image after 11 min (redisplayed from figure 2, for comparison). 1 μm wide scan

As this is imaging in the attractive regime no sample damage is expected. The images in figure S7, however, appear to get less and less sharp/well defined over time, this is interpreted as an effect of protein leaking out and coating the surface.

Time after PBS: 18min



Time after PBS: 23 min



Time after PBS: 28min

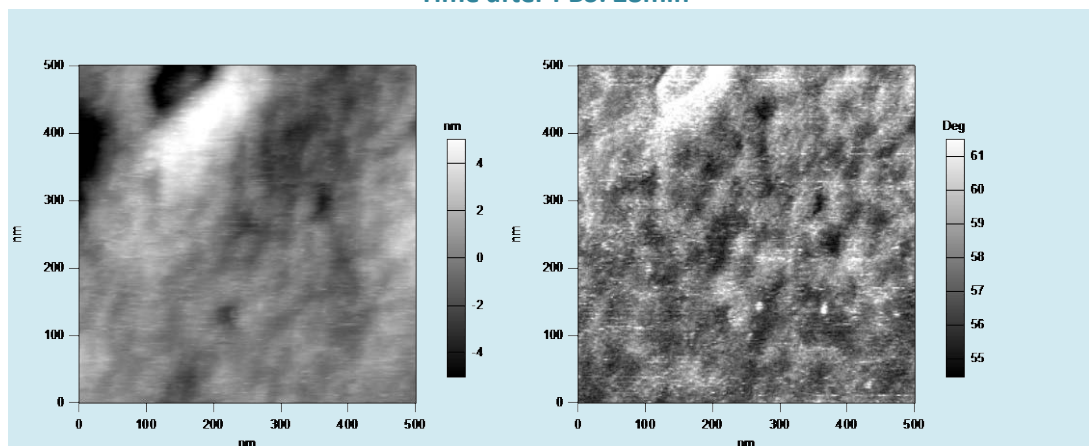


Figure S7: Initial height (left) and phase (right) images of 500 nm scans of PS-b-PEO Lsm α PEG (18-28 min after initial exposure to PBS).

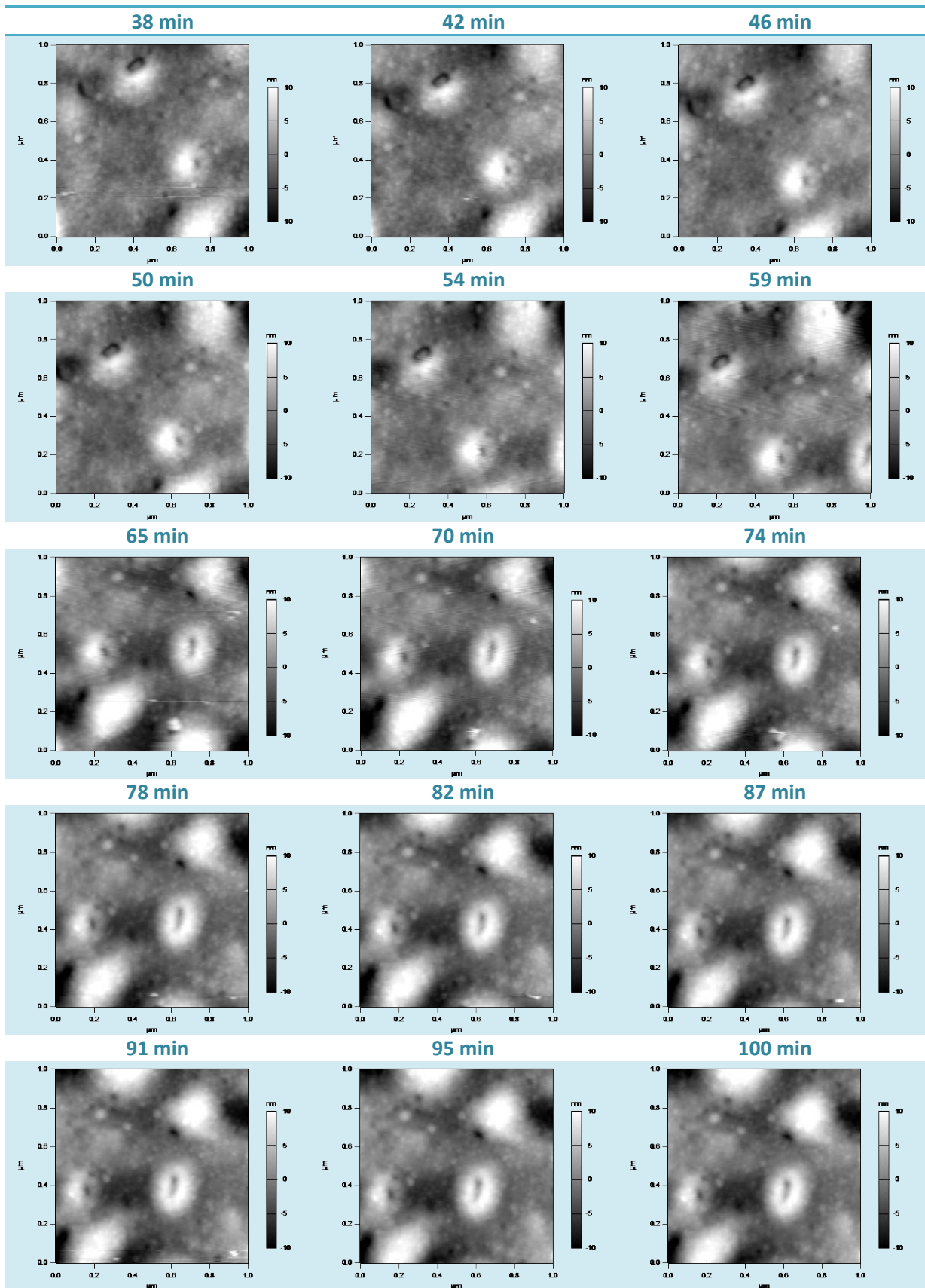


Figure S8: A series of scans in a slightly new area compared to Figure S7. Height images of 1 μm scans of PS-b-PEO Lsm α PEG 38-100 min after initial contact with buffer. Images have been plane fitted in X/Y and all images are displayed with a 20 nm height scale. Slight drift in imaging position occurs over the sequence, which lead to that the images move up and left in the frame over time.

Protein deposited on top of PS-b-PEO:

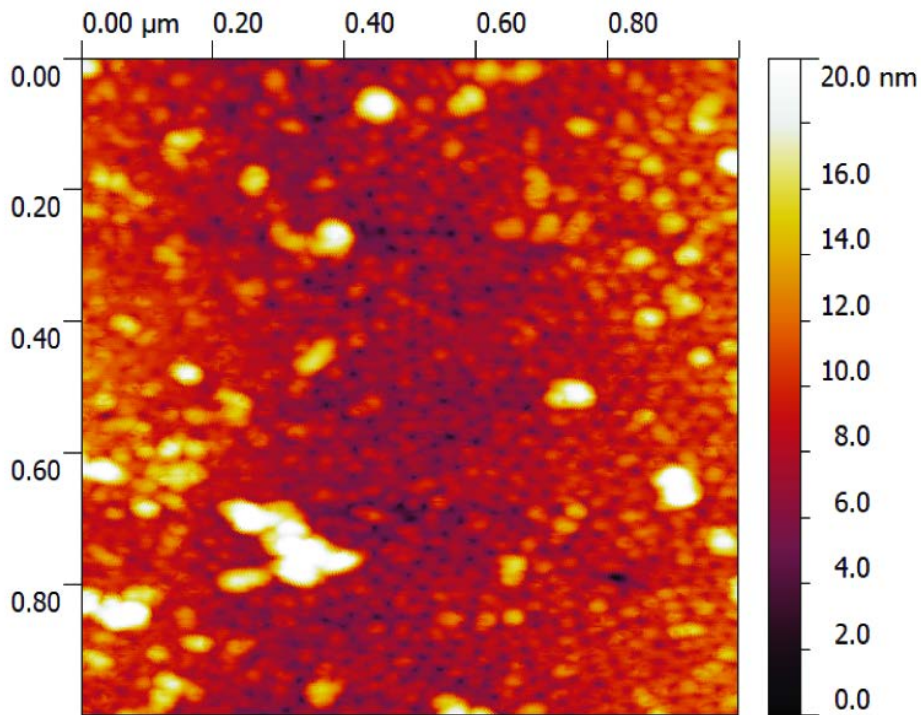


Figure S9: Lsm α adsorbed on top of PS-b-PEO and imaged in air by AFM.

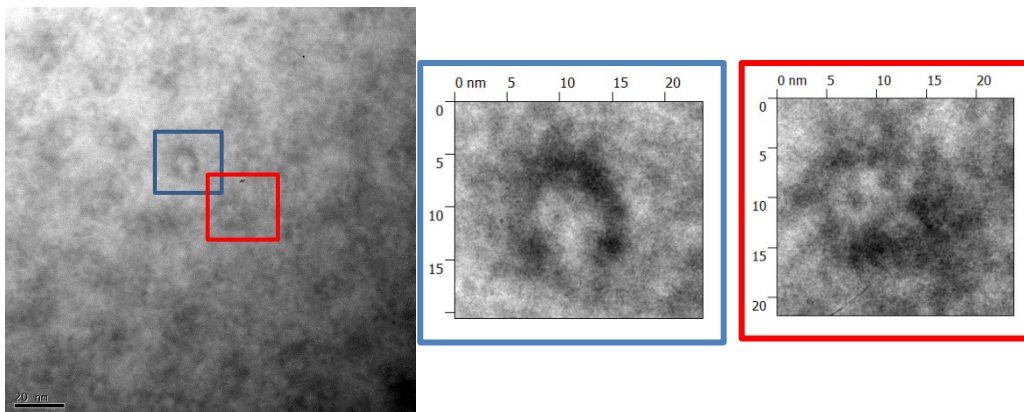


Figure S10: TEM of dipcoated PS-b-PEO/Lsm α /PEG stained with RuO₄ vapor. Zoomed in areas displaying PEO domains with protein inside.

The need for RuO₄ staining was explored by also imaging the films unstained (figure S11) and stained by uranyl acetate (figure S12). Uranyl acetate obscures some of the features of the surface, but remains a viable option, probably due to preferential wetting of the polystyrene. The unstained films exhibit enough contrast to see the hexagonal pattern, but are unstable under the beam. The

unstained image has an inversed contrast compared to the RuO₄ stained film, which is indicative of the lower electron density of the PEO vs the PS domains.

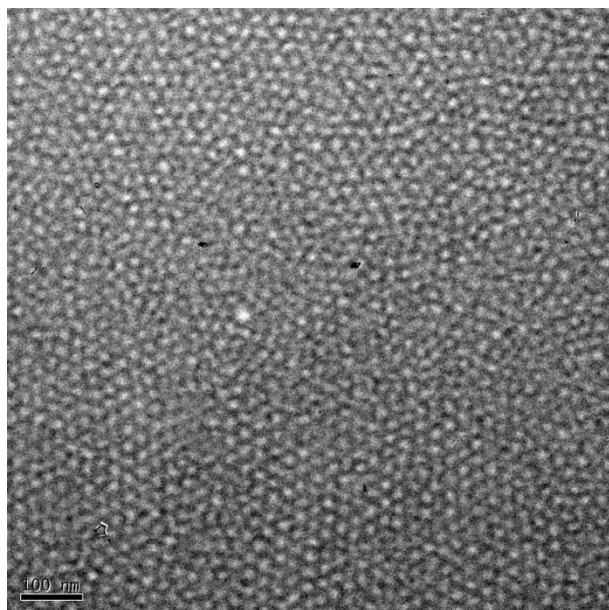


Figure S11: TEM image of PS-b-PEO spin coated on carbon coated mica and lifted to a Cu-grid. Unstained. Scalebar 100 nm.

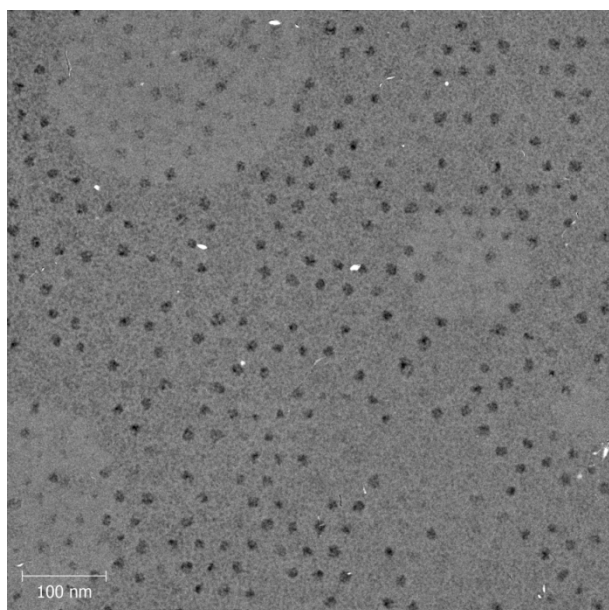


Figure S12: TEM image of PS-b-PEO Lsm α PEG, spin coated on carbon coated mica and lifted to Cu-grid. Stained with Uranyl acetate for 20 min. Scalebar 100 nm.

REFERENCES:

1. B. M. Collins, S. J. Harrop, G. D. Kornfeld, I. W. Dawes, P. M. G. Curmi and B. C. Mabbutt, *Journal of Molecular Biology*, 2001, **309**, 915-923.
2. C. J. Fee and J. M. Van Alstine, *Chemical Engineering Science*, 2006, **61**, 934-939.

3. C. Y. Zheng, G. Ma and Z. Su, *Electrophoresis*, 2007, **28**, 2801-2807.
4. M. F. Delcroix, E. M. Zuyderhoff, M. J. Genet and C. C. Dupont-Gillain, *Surface and Interface Analysis*, 2012, **44**, 175-184.
5. J. Malmstrom, H. Agheli, P. Kingshott and D. S. Sutherland, *Langmuir*, 2007, **23**, 9760-9768.
6. T. G. Flick, S. I. Merenbloom and E. R. Williams, *Journal of the American Society for Mass Spectrometry*, 2011, **22**, 1968-1977.

ⁱ1P (0.93%) and Si (0.89%)